

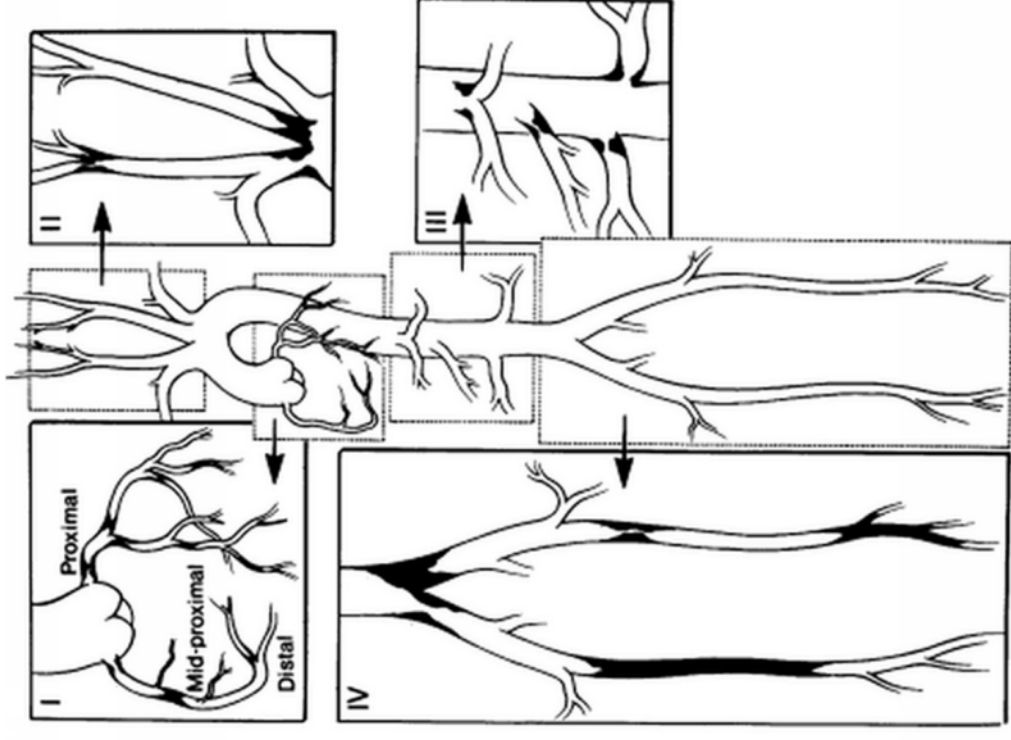
# Atherosclerosis and Fluid Mechanics

(or more generally,  
Atherosclerosis and  
Biomechanics)

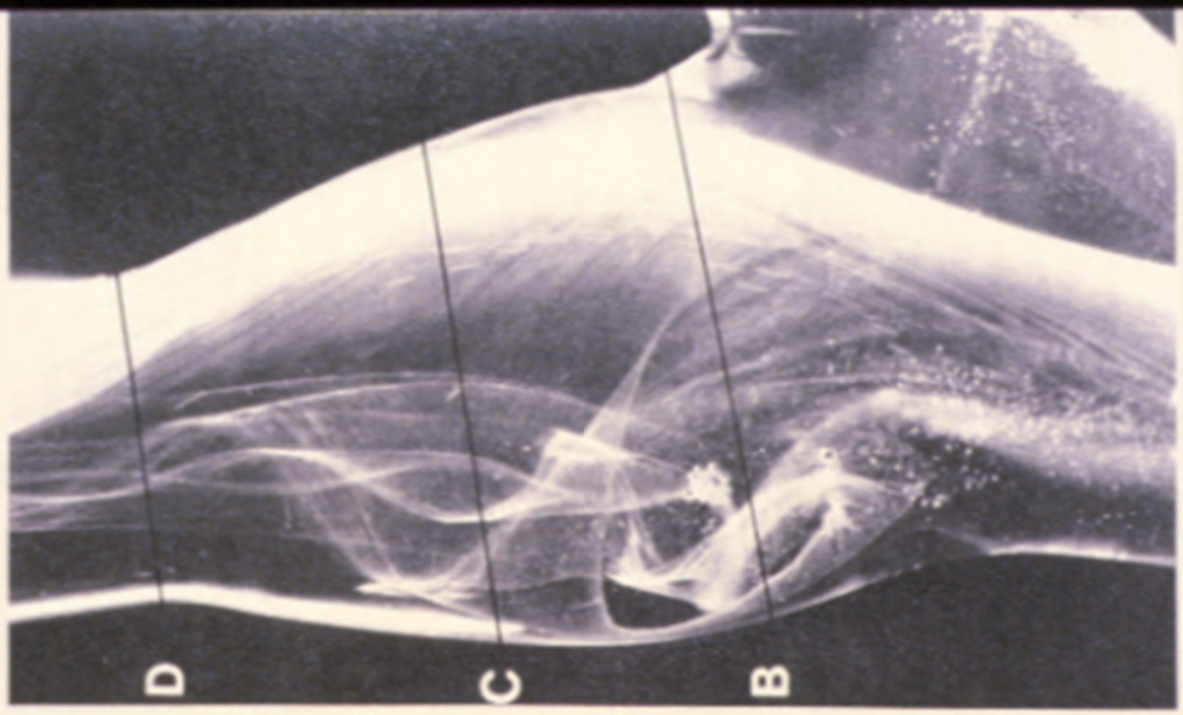
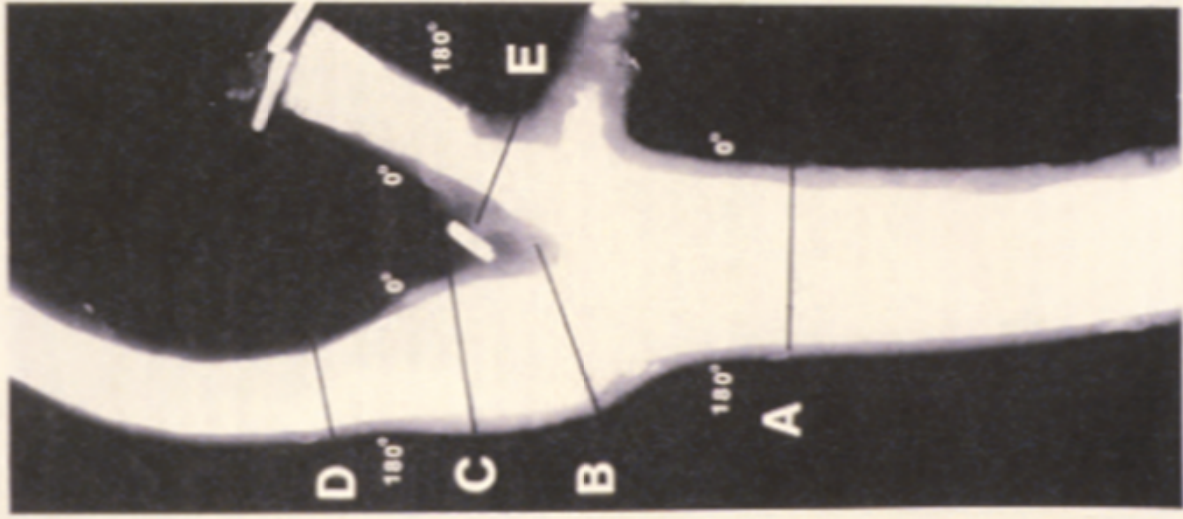
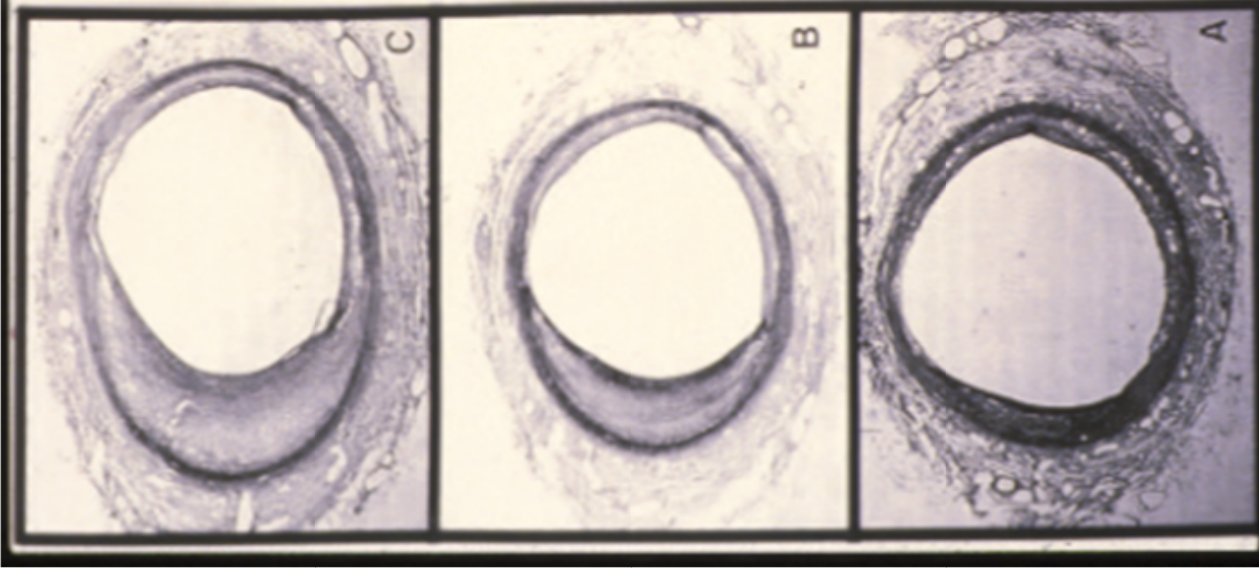
Ross Ethier  
r.ethier@imperial.ac.uk

# Facts about Atherogenesis

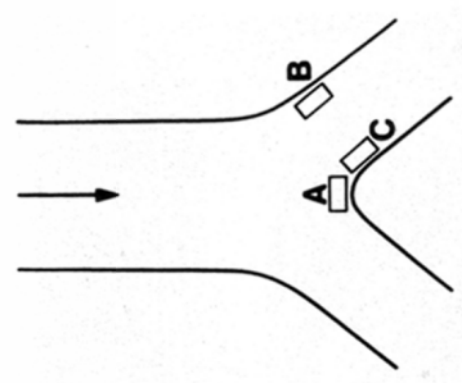
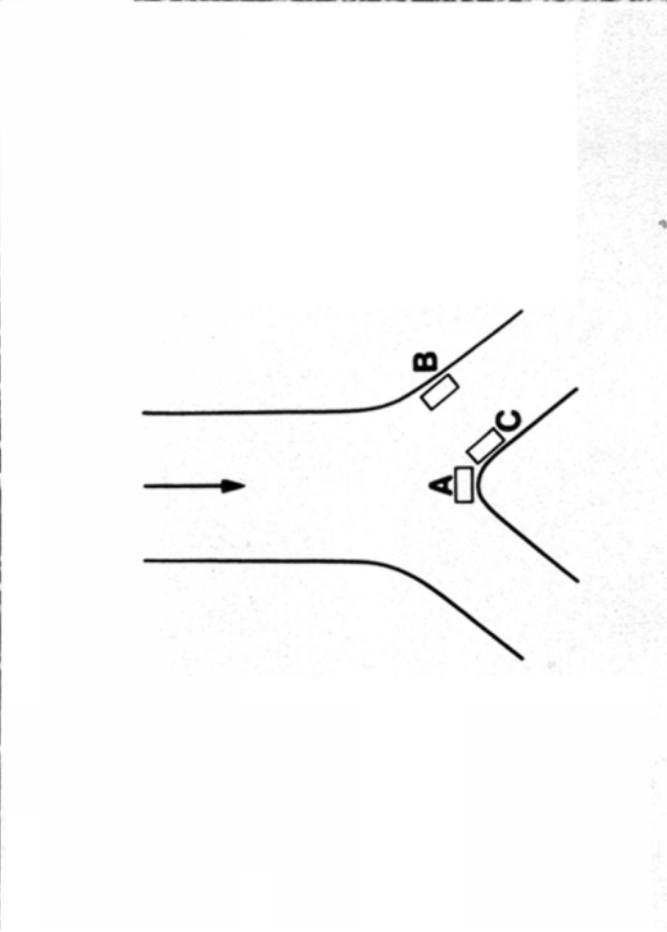
- Atherosclerosis is focal: “hot spots”.
- Regions of curvature and bifurcation are at risk.
- These are sites of “disturbed” hemodynamics.
- Biomechanical factors are strongly implicated in atherogenesis (“low and oscillatory shear stress”).



DeBakey et al, 1985



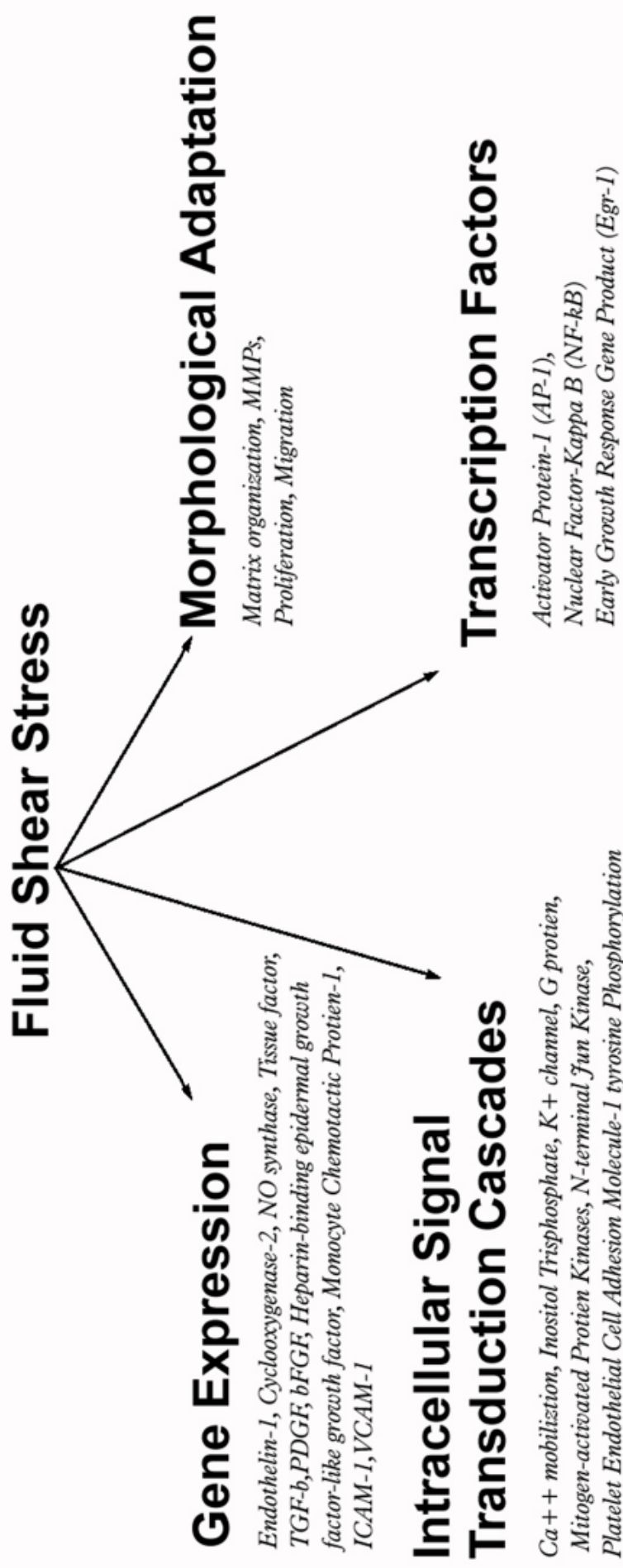
Zarins et al. Circ Res 1983



Kim et al. *Circ Res* 1989;64:21-31



# Fluid Shear Stress



## Gene Expression

*Endothelin-1, Cyclooxygenase-2, NO synthase, Tissue factor, TGF- $\beta$ , PDGF, bFGF, Heparin-binding epidermal growth factor-like growth factor, Monocyte Chemoattractant Protein-1, ICAM-1, VCAM-1*

## Morphological Adaptation

*Matrix organization, MMPs, Proliferation, Migration*

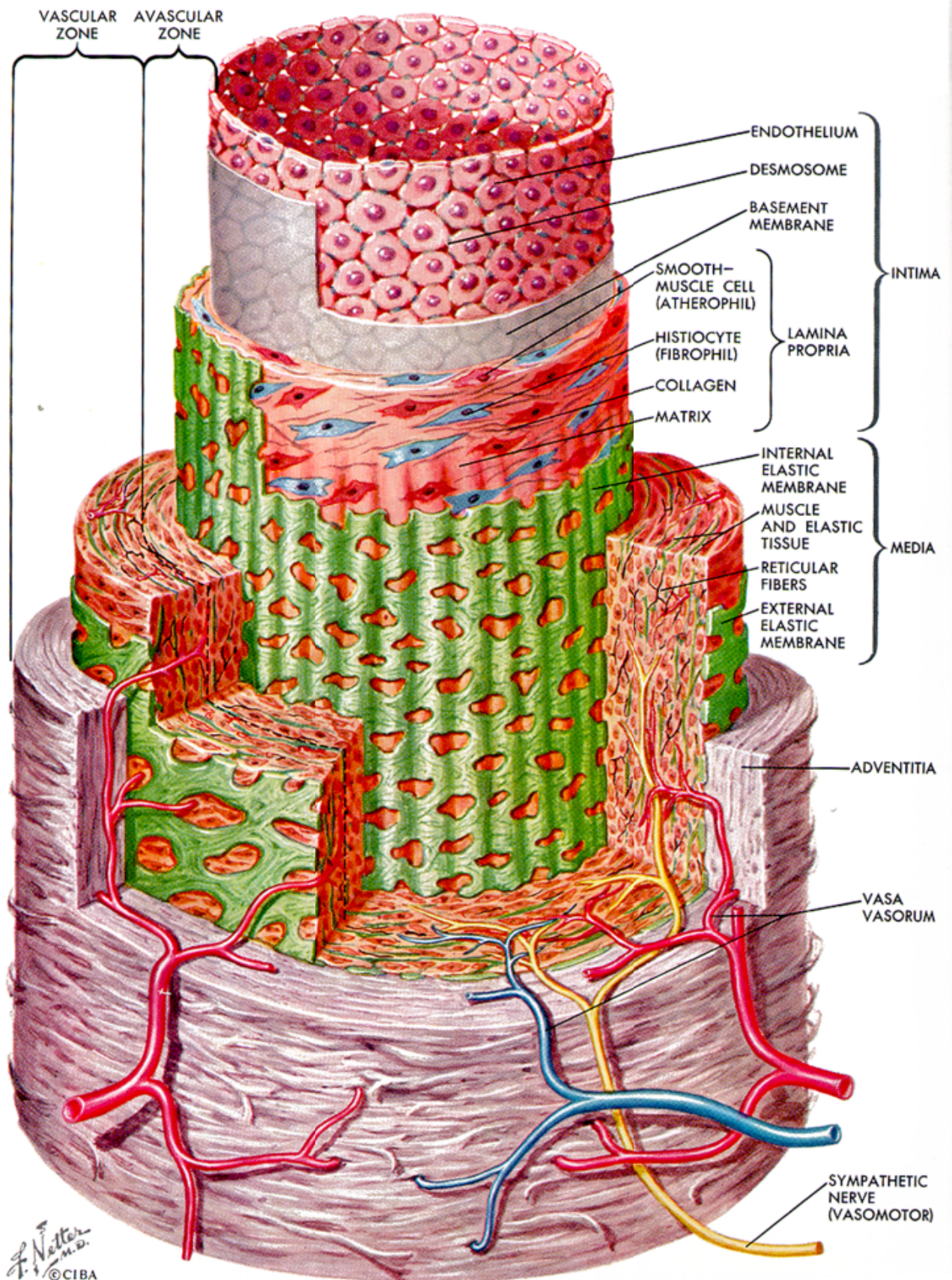
## Intracellular Signal

## Transduction Cascades

*Ca<sup>++</sup> mobilization, Inositol Trisphosphate, K<sup>+</sup> channel, G protein, Mitogen-activated Protein Kinases, N-terminal Jun Kinase, Platelet Endothelial Cell Adhesion Molecule-1 tyrosine Phosphorylation*

## Transcription Factors

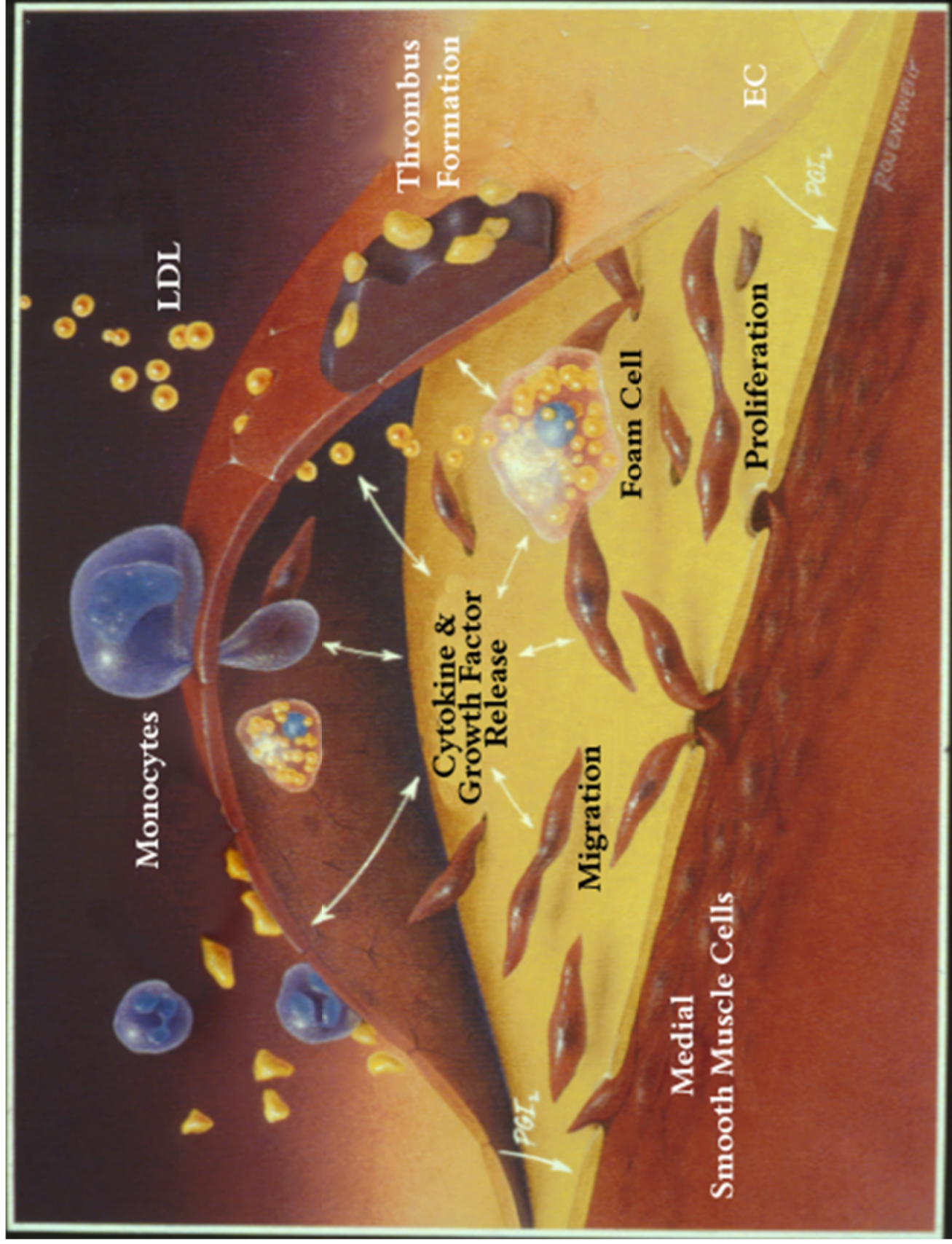
*Activator Protein-1 (AP-1), Nuclear Factor-Kappa B (NF- $\kappa$ B) Early Growth Response Gene Product (Egr-1)*



F. Netter M.D.  
© CIBA

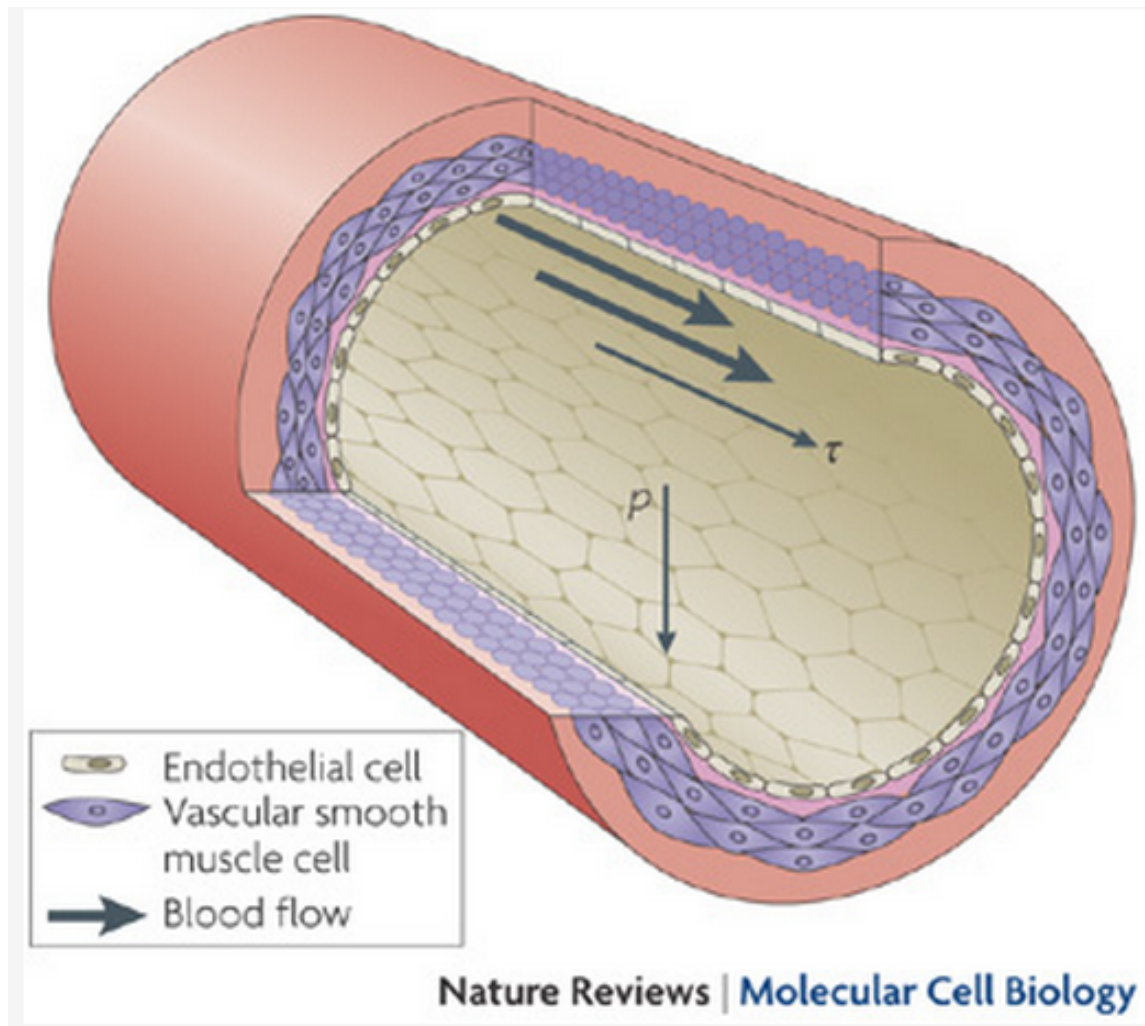


# Atherosclerosis



# Forces acting on the artery wall

Note that longitudinal tension is not shown!



A section of an artery wall shows the endothelial cells that form the inner lining and align longitudinally, and vascular smooth muscle cells that form the outer layers and align circumferentially. Pressure ( $p$ ) is normal to the vessel wall, which results in circumferential stretching of the vessel wall. Shear stress ( $\tau$ ) is parallel to the vessel wall and is exerted longitudinally in the direction of blood flow.

From: Mechanotransduction in vascular physiology and atherogenesis  
Cornelia Hahn & Martin A. Schwartz  
Nature Reviews Molecular Cell Biology 10, 53-62 (January 2009)



### 4.3.3 Arterial wall structure and elasticity

---

The artery wall is a three-layered structure (Figs. 2.57 and 4.15 [color plate]). The innermost (blood-contacting) layer is known as the *tunica intima*, and in a young, healthy artery is only a few micrometers thick. It consists of endothelial cells and their basal lamina, containing type IV collagen, fibronectin, and laminin. The endothelial cells have an important barrier function, acting as the interface between blood components and the remainder of the artery wall. The middle layer is the *tunica media*, which is separated from the intima by a thin elastin-rich

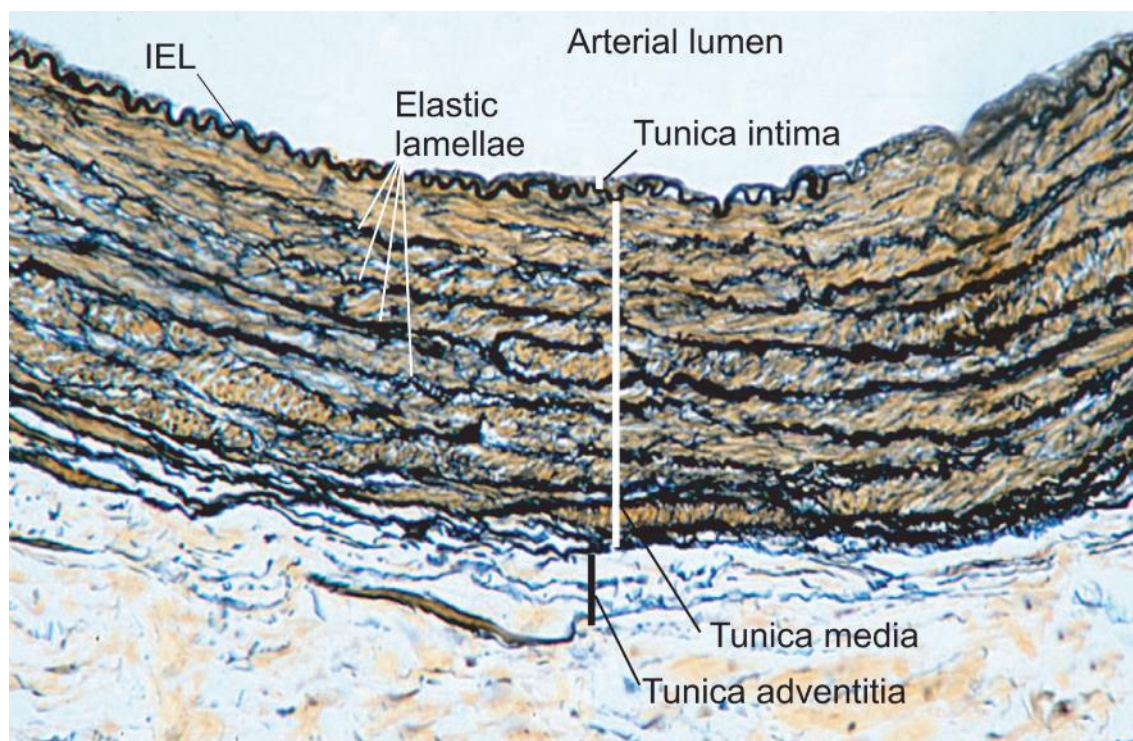


**Figure 4.15**  
Cross-section through the wall of an artery, demonstrating the tunicas intima, media, and adventitia, as well as elastic lamellae within the media. The elastin appears black in this preparation, which has been stained with Verhoeff's stain and lightly counter-stained to make the collagen appear blue. IEL, internal elastic lamina. Modified from Vaughan [19] by permission of Oxford University Press, Inc.

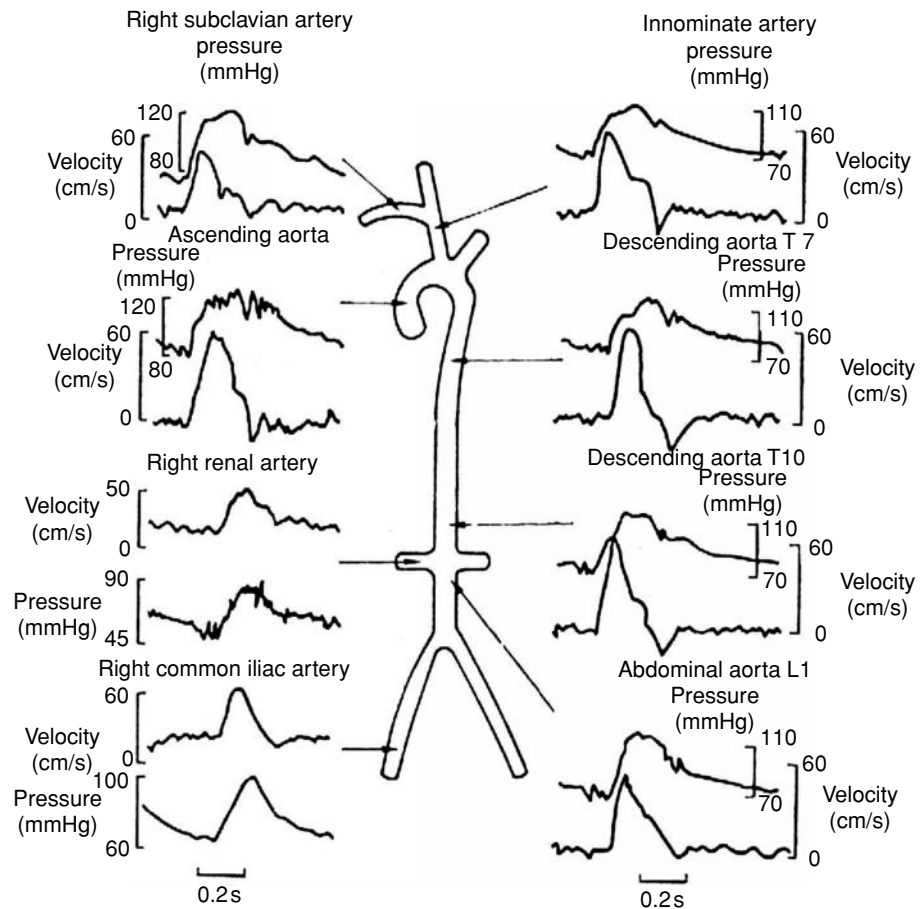


**Figure 4.14**

Simultaneous pressure and blood velocity waveforms at selected points in the human arterial tree. All waveforms were measured in the same patient except for those from the right renal artery and the right common iliac artery. Changes in the instantaneous pressure are approximate indicators of changes in arterial caliber, and thus of local blood storage. From Caro *et al.* [17], based on data reported in Mills *et al.* [18]. Reproduced with kind permission of Oxford University Press and the European Society of Cardiology.

ring known as the *internal elastic lamina*. The outermost layer is known as the *tunica adventitia*, which is separated from the media by the *outer elastic lamina*. The adventitia is a loose connective tissue that contains type I collagen, nerves, fibroblasts, and some elastin fibers. In some arteries, the adventitia also contains a vascular network called the *vasa vasorum*, which provides nutritional support to the outer regions of the artery wall. Biomechanically, the adventitia helps to tether the artery to the surrounding connective tissue.

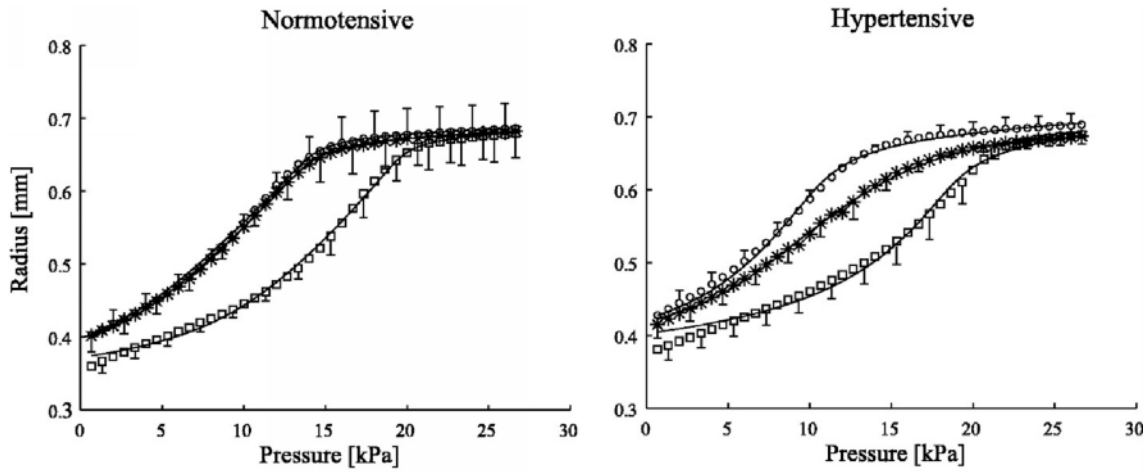


**Figure 4.16**

Pressure–radius relationship for the carotid arteries of normotensive and hypertensive rats measured under static conditions. The symbols are experimental measurements averaged over six or more rats, the error bars represent standard deviation, and the lines are the fit of a constitutive model to the experimental data. Each graph has three datasets with different vascular smooth muscle (VSM) tone: fully relaxed VSM ( $\circ$ ), normal VSM tone ( $*$ ), and maximally contracted VSM ( $\square$ ). It can be seen that the state of the vascular smooth muscle has a profound effect on the mechanical properties of the artery wall, and that the contribution of vascular smooth muscle is different in normotensive and hypertensive arteries. Reproduced from Zulliger *et al.* [20] with permission of the American Physiological Society.

The media is the most important layer for determining the biomechanical properties of the artery wall. It contains smooth muscle cells, elastin, types I, III, and V collagen, and proteoglycans. Smooth muscle cells are oriented circumferentially and, as can be seen from Fig. 4.16, have an important influence on arterial stiffness, especially in the smaller arteries. They also provide control of arterial caliber. The collagen is oriented largely circumferentially [21] with a slight helical pattern. The relative proportion of elastin to collagen changes with position in the vascular tree: in the dog, the proportion of elastin in the thoracic aorta is about 60%, but this value decreases significantly near the diaphragm and then gradually falls to about 20% for the peripheral arteries [8]. As elastin content falls, smooth muscle content increases, and arteries are, therefore, classified as being either *elastic* (the large central arteries) or *muscular* (the smaller peripheral arteries).

As we will see in Chapter 9, most biological materials demonstrate highly non-linear stress–strain behavior, and the artery wall is no exception. Figure 4.16 shows pressure–radius data gathered from static inflation tests on excised rat carotid arteries. In these tests, a segment of artery is excised and mounted on a test apparatus that allows the artery lumen to be pressurized while the artery is bathed in a physiological saline solution. The outer arterial diameter is then measured as the luminal pressure is increased. For a linearly elastic, thin-walled artery undergoing



small deformations, a linear pressure–radius relationship is expected. It can be seen from the data in Fig. 4.16 that a linear relationship is not present, with the artery experiencing significant stiffening as the luminal pressure exceeds approximately 15 kPa (110 mmHg) in the relaxed state. This reflects the strain-stiffening behavior of the collagen and elastin in the artery wall.

In addition to its non-linearity, the artery wall is anisotropic (stiffness is different in different directions) and viscoelastic. Therefore, it is not possible to characterize the stiffness of a given artery wall completely by a single number, such as a Young’s modulus. Nonetheless, it is possible to make operational measurements of the stiffness of the artery by observing the change in outer radius,  $\Delta R_o$ , as the luminal pressure is varied. This leads to a quantity called the “pressure–strain” modulus,  $E_p$ , defined by [22]

$$E_p = R_o \frac{\Delta p}{\Delta R_o}, \quad (4.15)$$

where  $R_o$  is the average outer radius of the artery as the pressure is changed by  $\Delta p$ . Measured values of this quantity for arteries in humans are shown in Table 4.2.

Based on work by Bergel for the distension of an isotropic, thick-walled elastic tube (see summary in Milnor [4]), Gow and Taylor [29] related  $E_p$  to the incremental Young’s modulus for the artery wall,  $E_{inc}$ , by the expression

$$E_{inc} = E_p \frac{2(1 - \nu^2) \left(1 - \frac{t}{R_o}\right)^2}{1 - \left(1 - \frac{t}{R_o}\right)^2} \quad (4.16)$$

where  $t$  is artery wall thickness and  $\nu$  is Poisson’s ratio. This should be interpreted as a circumferential elastic modulus:  $E_{\theta\theta}$ . The value of the ratio  $t/R_o$  depends on age and increases with distance from the heart, but a typical value for humans aged 36–52 years is approximately 0.15 [8]. Using this value, as well as a Poisson’s ratio of 0.5, we compute from Equation (4.16) that  $E_{inc} \approx 4E_p$ . Using this, as well as the values in Table 4.2, we see that incremental Young’s modulus values range from about  $3 \times 10^6$  to  $20 \times 10^6$  dynes/cm<sup>2</sup> for the systemic arteries. A more careful analysis, accounting for variations in wall thickness with position, gives elastic modulus values between  $8 \times 10^6$  and  $25 \times 10^6$  dynes/cm<sup>2</sup> [8]. Numerous constitutive relationships for vessel walls have been developed and have been summarized by Vito and Dixon [30].

**Table 4.2. Values of the “pressure–strain modulus”,  $E_p$ , and other arterial parameters in humans. From more complete listings in Milnor [4] and Nichols and O’Rourke [8], except the values for aortic root.**

Artery	No. <sup>a</sup>	$R_0$ (cm) <sup>b</sup>	Pressure (mmHg) (mmHg)	Radial pulsation (%) <sup>c</sup>	$E_p$ (dyn/cm <sup>2</sup> ) <sup>d</sup>	Source
Aortic root <sup>e</sup>	1	1.6	–	±4.7	–	Jin <i>et al.</i> [23]
Ascending aorta	10	1.42	79–111	±2.9	$0.76 \times 10^6$	Patel and Fry [24]
Thoracic aorta	12	1.17	98–174	±2.6	$1.26 \times 10^6$	Luchsinger <i>et al.</i> [25]
Femoral	6	0.31	85–113	±0.6	$4.33 \times 10^6$	Patel <i>et al.</i> [24]
Carotid	11	0.44	126–138	±0.5	$6.08 \times 10^6$	Patel <i>et al.</i> [24]
Carotid	16	0.40	96	±7.4	$0.49 \times 10^6$	Arndt [26]
Carotid	109	–	–	–	$0.63 \times 10^6$	Riley <i>et al.</i> [27]
Pulmonary (main)	8	1.35	16	±5.6	$0.16 \times 10^6$	Greenfield and Griggs [28]
Pulmonary (left)	5	1.07	25	±6.2	$0.17 \times 10^6$	Luchsinger <i>et al.</i> [25]
Pulmonary (right)	13	1.13	27	±5.8	$0.16 \times 10^6$	Luchsinger <i>et al.</i> [25]
Pulmonary (main)	8	1.43	18–22	±5.4	$0.16 \times 10^6$	Patel <i>et al.</i> [24]

<sup>a</sup> Number of arteries studied.

<sup>b</sup> Mean outer radius.

<sup>c</sup> Pulsation about the mean radius from normal pulse pressures (i.e.,  $100 \times$  one-half the total radial excursion in each cardiac cycle (systolic–diastolic) divided by the average radius).

<sup>d</sup> Calculated from Equation (4.15) using total excursion of pressure and radius during natural pulsations; therefore represents a dynamic modulus.

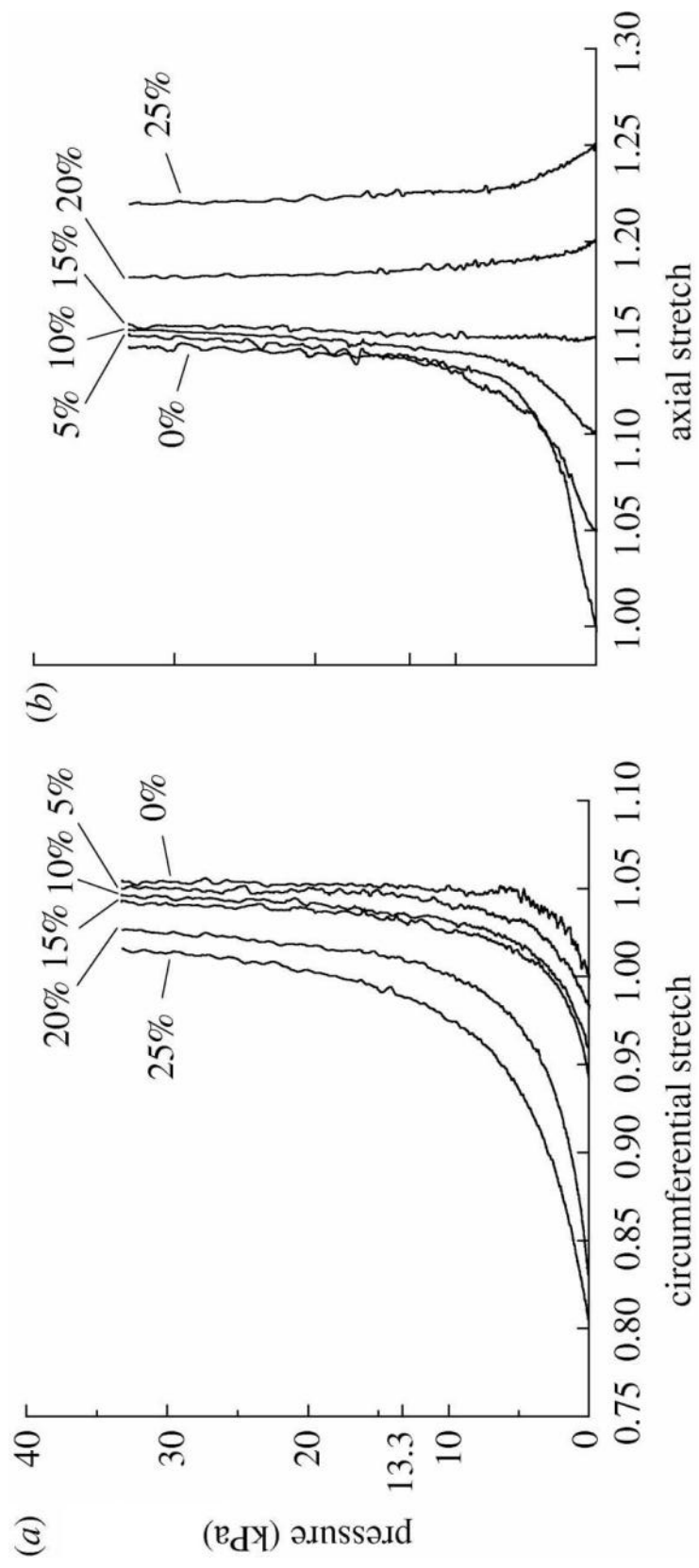
<sup>e</sup> Measured using MRI.

Can table heading entries be botom justified? (Here and in all tables).

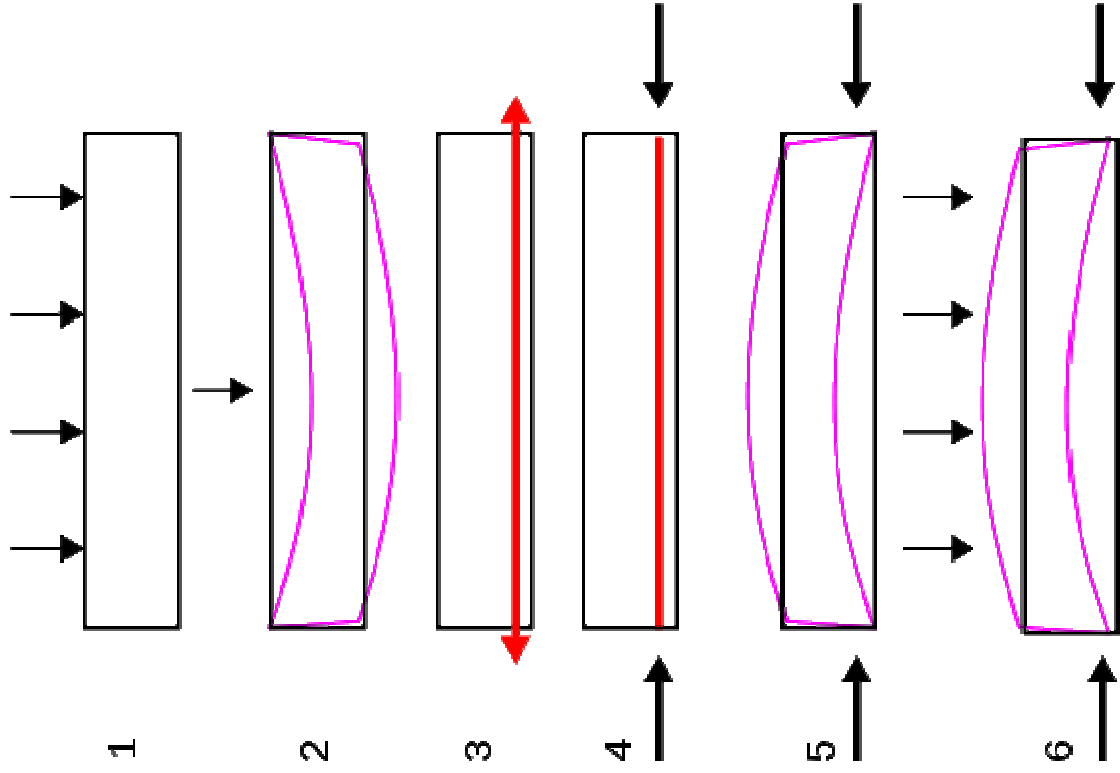
# Representative pressure–stretch response of an intact internal carotid artery.

Inflation behaviour depends on axial stretch

Arteries lengthen/shorten as they are pressurised



Holzapfel G A , Ogden R W Proc. R. Soc. A  
doi:10.1098/rspa.2010.0058



# PRESTRESSED CONCRETE

A FUNDAMENTAL APPROACH  
FIFTH EDITION



EDWARD G. NAWY



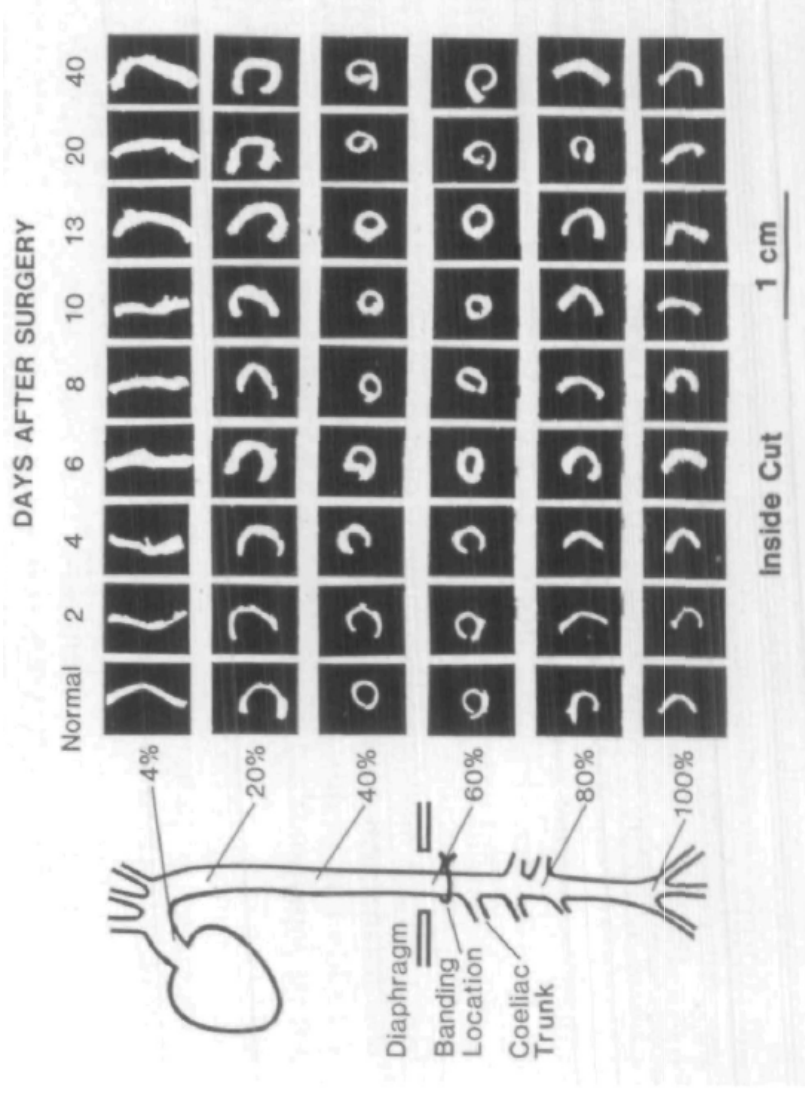


FIGURE 2. Photographs of the cross sections of the aorta when cut first transversely and then radially along the "inside" line indicated in Figure 1. Listing is arranged according to days after surgery from left to right, and according to location on the aorta from top to bottom, expressed as distance from the heart in percentage of total length. Location of the metal clip is shown in sketch at left. Arcs of the blood vessel wall do not appear smooth because some tissue was attached to the wall. In reading these photographs, one should mentally delete these tethered tissues.

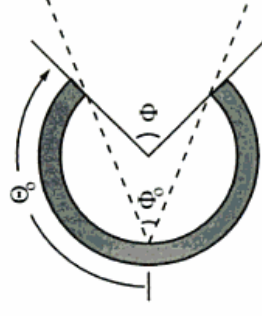


Image from Cardiovascular solid mechanics: cells, tissues, and organs, by JD Humphrey

- Opening angle (and hence residual stress) depends on position
- Opening angle is affected by blood pressure (banding surgery increased aortic BP)

Change of residual strains in arteries due to hypertrophy caused by aortic constriction

YC Fung and SQ Liu  
*Circ. Res.* 1989;65:1340-1349

Strain is uniform across the artery wall when residual strains are taken into account (artery “wants” a uniform environment across the wall)

TABLE 7.3. Comparison of circumferential stretch at the intimal and adventitia surfaces between cases when residual strains are ignored versus included

Vessel	State	Based on stress-free		Based on unloaded state	
		Intimal	Adventitial	Intimal	Adventitial
Ileal	Stress-free	1.0	1.0	—	—
	Unloaded	0.79	1.13	1.0	1.0
	80 mm Hg	1.37	1.33	1.72	1.17
Pulmonary	120 mm Hg	1.38	1.34	1.73	1.18
	Stress-free	1.0	1.0	—	—
	Unloaded	0.70	1.28	1.0	1.0
	10 mm Hg	1.34	1.47	1.92	1.14
	15 mm Hg	1.40	1.50	2.01	1.17

From Liu and Fung (1992).

From Humphrey, “Cardiovascular solid mechanics: cells, tissues, and organs”

# Hypertension-induced remodelling

Biomechanics of the Porcine Basilar Artery in Hypertension  
J.-J. Hu, T. W. Fossum, M. W. Miller, H. Xu, J.-C. Liu and J. D. Humphrey  
Annals of Biomedical Engineering (2006)

## Methods

- Studied basilar arteries of minipigs
- Hypertension induced by aortic coarctation
- Arteries excised and tested for:
  - mechanical properties,
  - wall thickness and
  - lumen diameter

Hypertension (HT) leads to a thicker wall and more collagen than in normotensive (NT) arteries

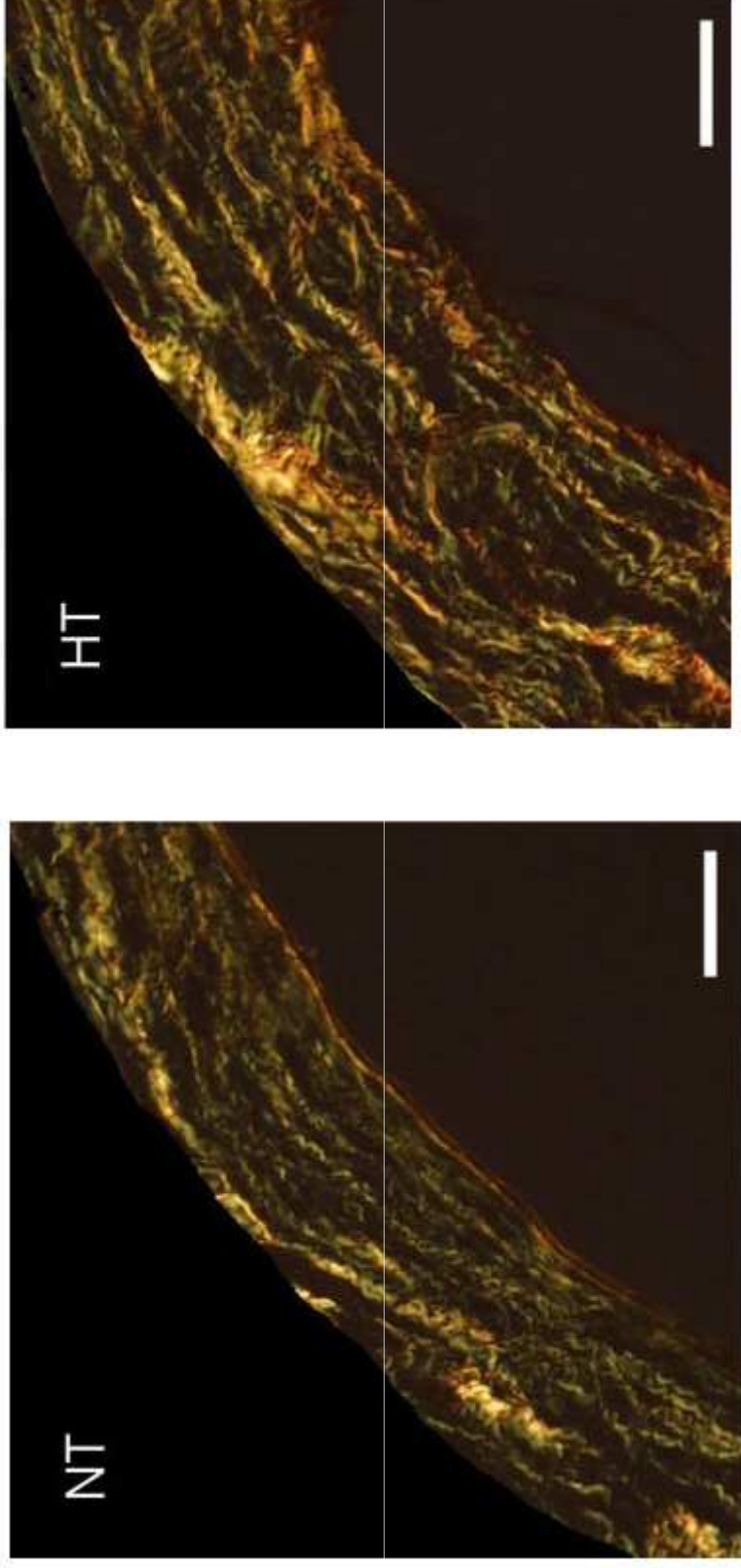
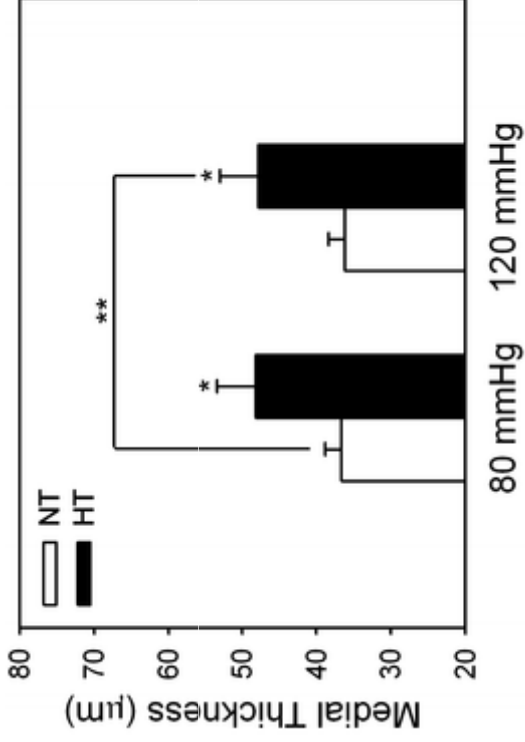


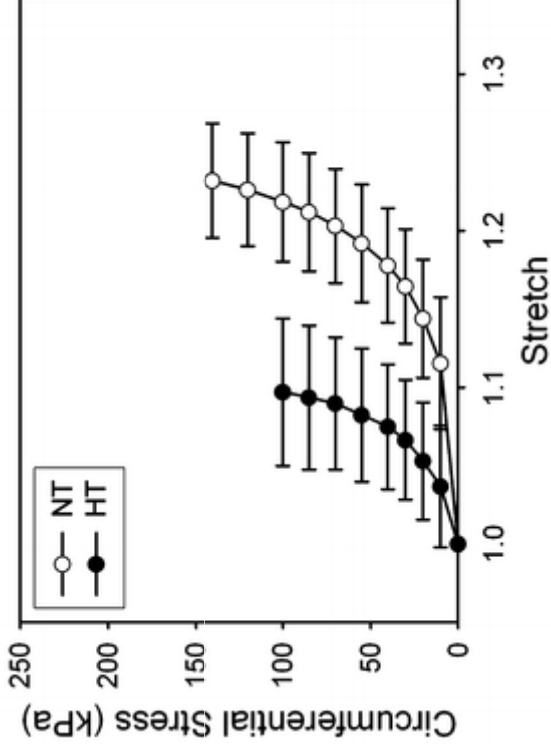
**Figure 6.** Illustrative picosirius red (PSR) stained cross-sections of the media of basilar arteries from NT (top) and HT (bottom) mini-pigs viewed under circularly polarized light. The specimens were fixed in the unloaded condition. Although somewhat difficult to discern by eye, computer analysis revealed a significant (30%) increase in medial collagen due to hypertension. The scale bar is 25  $\mu\text{m}$



Media thickens in hypertension (HT)

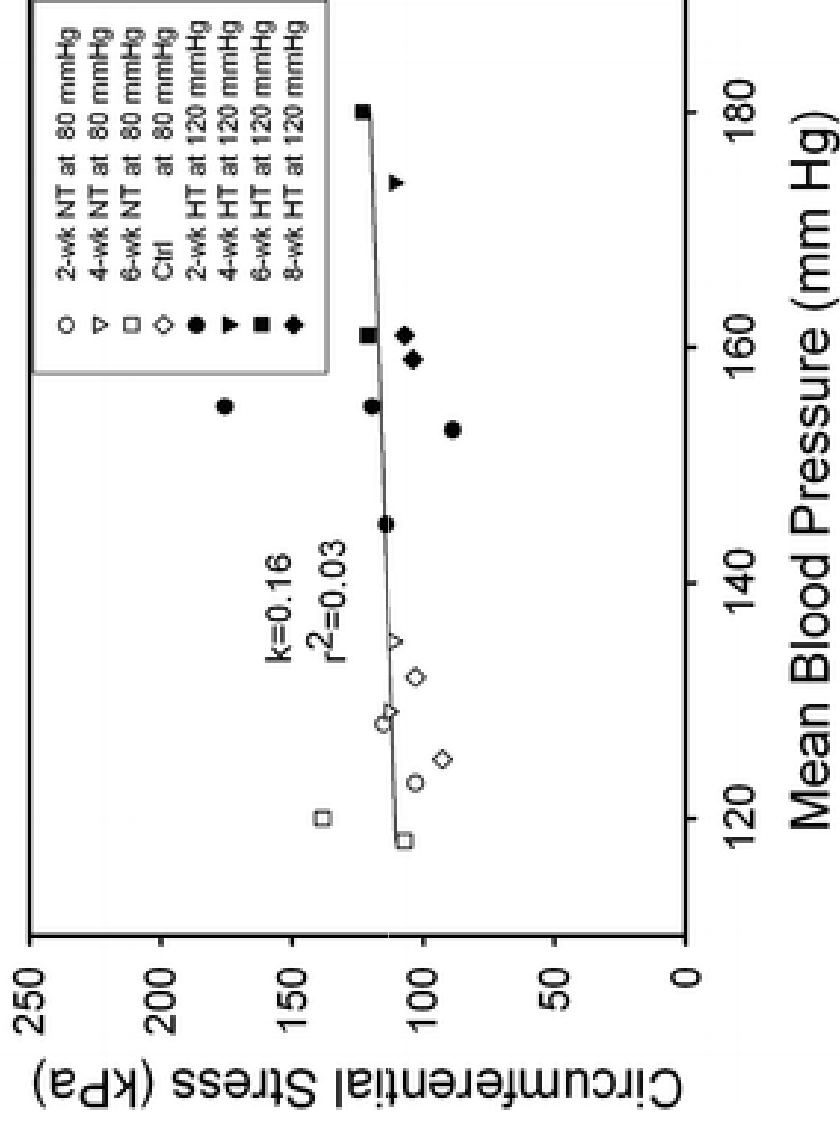


And the wall gets stronger



Biomechanics of the Porcine Basilar Artery in Hypertension  
J.-J. Hu, T. W. Fossom, M. W. Miller, H. Xu, J.-C. Liu and J. D. Humphrey  
Annals of Biomedical Engineering (2006)

# Artery remodels to reach a “target” circumferential stress



Biomechanics of the Porcine Basilar Artery in Hypertension  
 J.-J. Hu, T. W. Fossom, M. W. Miller, H. Xu, J.-C. Liu and J. D. Humphrey  
 Annals of Biomedical Engineering (2006)

the  $\alpha$  is the Womersley parameter (Section 3.2.3);  $Re_D$  is the Reynolds number (based on vessel diameter) given as mean with peak value in parentheses. Values collated from a variety of sources by Milnor [17]. Reproduced with kind permission of Lippincott Williams & Wilkins.

	Dog			Human		
	$\alpha$	Velocity (cm/s) <sup>a</sup>	$Re_D$	$\alpha$	Velocity (cm/s) <sup>a</sup>	$Re_D$
<i>Systemic vessels</i>						
Ascending aorta	16	15.8 (89/0)	870 (4900)	21	18 (112/0)	1500 (9400)
Abdominal aorta	9	12 (60.0)	370 (1870)	12	14 (75/0)	640 (3600)
Renal artery	3	41 (74/26)	440 (800)	4	40 (73/26)	700 (1300)
Femoral artery	4	10 (42/1)	130 (580)	4	12 (52/2)	200 (860)
Femoral vein	5	5	92	7	4	104
Superior vena cava	10	8 (20/0)	320 (790)	15	9 (23/0)	550 (1400)
Inferior vena cava	11	19 (40/0)	800 (1800)	17	21 (46/0)	1400 (3000)
<i>Pulmonary vessels</i>						
Main artery	14	18 (72/0)	900 (3700)	20	19 (96/0)	1600 (7800)
Main vein <sup>b</sup>	7	18 (30/9)	270 (800)	10	19 (38/10)	800 (2200)

<sup>a</sup> Velocities are temporal means with systolic/diastolic extremes in parentheses.

<sup>b</sup> One of the usually four terminal pulmonary veins.

downstream of severe stenoses [26]. The values in Table 3.6 are averages; it can be appreciated from the range of reported values in Table 3.7 that significant variation from one person to the next is typical.

**Table 3.7. Comparison of hemodynamic parameters in selected arteries in humans.  $Q$ , mean (cycle-averaged) flow rate in ml/s;  $D$ , cycle-averaged diameter in mm;  $U_0$ , mean (cycle-averaged) velocity in cm/s;  $Re_D$ , Reynolds number based on  $D$ ,  $U_0$  and an assumed blood kinematic viscosity of 3.5 cStokes;  $\tau$ , mean wall shear stress determined from  $\tau = 8\mu U_0/D = 32 \mu Q/\pi D^2$ , in dyne/cm<sup>2</sup> (this formula for shear stress ignores approximately 10% error from mean flow–pulsatile interactions). Reproduced from Ethier *et al.* [12] with permission from WIT Press, Southampton, UK.**

Artery	$Q$	$D$	$U_0$	$Re_D$	$\tau$	Comment and source
Common carotid <sup>a</sup>	6.0	6.3	19.3	347	8.6	Ultrasonography on young healthy volunteers (D. Holdsworth, unpublished communication, 1996)
	8.7	7.3	20.7	432	7.9	Ultrasonography on 47 healthy volunteers [18]
	7.5	7.3	17.9	373	6.9	Doppler (flow) [18] and 2 transducer (diameter) [19] ultrasonography on 35 normals
		8.2				Milnor, Table 4.3 [17]
Superficial femoral <sup>b</sup>	2.2	6.5	6.6	125	2.9	Color and B-mode ultrasonography, scaled to match graft flow rates [20]
	2.2	6.6	6.4	121	2.7	Ultrasonography on 4 healthy volunteers [18]
	5.2	6.5 <sup>c</sup>	15.7	291	6.8	Doppler ultrasonography after balloon angioplasty [21]
	3.6	6.2	12.0	212	5.4	Catheter tip velocity probe (Milnor [17], Tables 4.3 and 6.3)
Thoracic aorta	45–93	23–28	8.9–18.4	640–1330	1.0–2.0	Biplanar angiography & cadaver specimens [22,23] <sup>d</sup>

<sup>a</sup> Ignores flow entrance effects, but entrance length = 0.06  $Re_D = 24$  diameters, so this is a small effect. Compare with mean wall shear stress of 7 dyne/cm<sup>2</sup> quoted in Ku *et al.* [10]

<sup>b</sup> First flow rate is suitable for diseased patients so is a lower bound for normals.

<sup>c</sup> Assumed value.

<sup>d</sup> Compare with mean wall shear stress of 1.3 dyne/cm<sup>2</sup> quoted in Ku and Zhu [24].

### 3.2.2 Steady blood flow at low flow rates

Although the non-Newtonian rheology of blood is not of primary importance in most arteries, it is important at lower shear rates, for example such as might occur at low flow rates in veins or in extracorporeal blood-handling systems. Here we

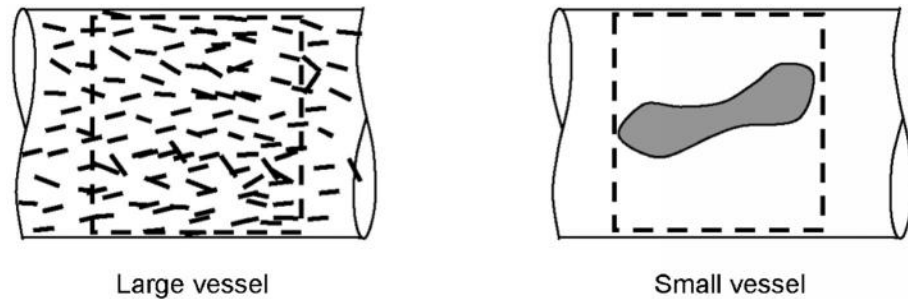


**Figure 3.9**

Schematic of red cells in large and small vessels. Note the relative size of red cells and control volumes (dotted lines).

consider this low shear case, and use the Casson constitutive relationship to derive the velocity profile for steady flow of blood in a large vessel or tube. It is recognized that blood flow is unsteady within the cardiovascular system, and the question may then be asked: What is the utility of studying steady flow of blood? The answer is threefold. First, steady blood flow can occur in extracorporeal blood-handling systems. Second, study of steady flow gives further insight into the importance of non-Newtonian rheology without involving a great deal of mathematical complication. Finally, pulsatile blood flow can be decomposed into a steady component and a zero mean-flow oscillatory component, and the following analysis addresses the steady component.

the  $\lambda$

A second question may be posed. Why restrict attention to flow in a large vessel or tube? Implicit in  $\lambda$  use of Casson rheology to model blood is the assumption that the fluid is a homogeneous continuum. This is true to a very good approximation in large vessels, since the red cells are very much smaller than the vessel diameter. In other words, on the scale of the vessel, the blood “looks” homogeneous, and we can therefore average red cell effects over a control volume (Fig. 3.9), much as is done in considering the continuum assumption in basic fluid mechanics. However, this is not true in, for example, capillaries, where red cells occupy a substantial fraction of the vessel.<sup>4</sup> We see from the above discussion that a “large” vessel in this context means a vessel with diameter “many times the size of a red cell,” for example 100 times larger than a red cell.

In vivo, vessels have complex shapes, exhibiting branching and curvature. However, their essential nature is that they are tubes; consequently, as a crude first approximation, it is acceptable to treat a vessel as a uniform cylinder. Hence, we will restrict our attention to the steady laminar flow of blood in a long straight tube, and ask: What is the velocity profile in such a flow? Mathematically, we denote the

<sup>4</sup> This is another bizarre aspect of suspension rheology: flow patterns can be dependent on the particle volume fraction, shear rate, and vessel size.



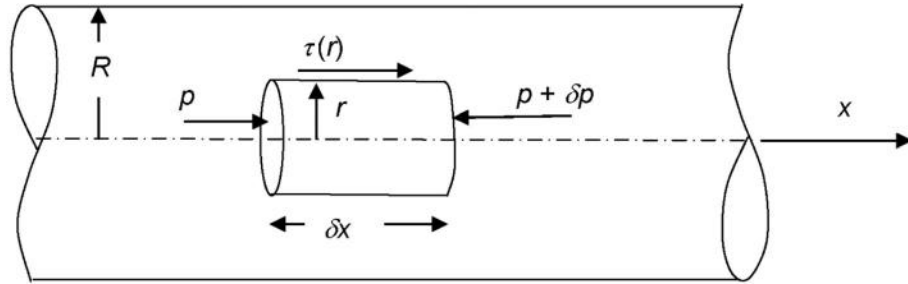


**Figure 3.10**

Forces acting on a small element of fluid for steady, fully developed flow in a tube of radius  $R$ .

axial velocity by  $u$  and the radial position by  $r$ , and seek an explicit representation of  $u(r)$ .

At this point it is worth recalling the shear stress distribution for steady, fully developed flow in a long straight tube of radius  $R$ . Considering a fluid element of length  $\delta x$  and radius  $r$ , we identify the following forces acting on that element: a pressure force  $p\pi r^2$  on the left face, a pressure force  $(p + \delta p)\pi r^2$  on the right face, and a shearing force  $\tau(r)2\pi r\delta x$  on the outer face (Fig. 3.10). Taking account of directions, and noting that for steady fully developed flow all fluid elements must experience zero acceleration and, thus by Newton's second law, zero net force, we may write

$$p\pi r^2 + \tau(r)2\pi r\delta x - (p + \delta p)\pi r^2 = 0. \quad (3.7)$$

Taking the limit as  $\delta x$  goes to zero, in which case  $\delta p/\delta x$  becomes the axial pressure gradient, we obtain:

$$\tau(r) = \frac{r}{2} \frac{dp}{dx}. \quad (3.8)$$

Note that this result is valid for all types of fluid, since it is based on a simple force balance without any assumptions about fluid rheology (see Box 3.1).

### Box 3.1 Using Equation (3.8) to derive Poiseuille's law for a Newtonian fluid

Since Equation (3.8) is valid for any type of fluid undergoing steady, fully developed flow, it can be used to derive Poiseuille's law for a Newtonian fluid. For such a fluid,  $\tau = \mu(du/dr)$  and Equation (3.8) becomes

$$\frac{1}{r} \frac{du}{dr} = \frac{1}{2\mu} \frac{dp}{dx}. \quad (3.9)$$

Now notice that the right-hand side of Equation (3.9) can only be a function of  $x$  (the pressure must be uniform on cross-sections of the tube or a non-axial component of the velocity would be generated), while for a fully developed flow the left-hand side can only be a function of  $r$ . The only way that a function of  $r$  can equal a function of  $x$  is if the function is a constant: that is, the two sides of Equation (3.9) must be constant. This means that the pressure gradient is a constant. Integrating Equation (3.9) once with respect to  $r$  and requiring the velocity to be zero at the wall and to be symmetric about the center line, we obtain the well-known parabolic velocity profile:

$$u(r) = -\frac{dp}{dx} \frac{R^2}{4\mu} \left[ 1 - \frac{r^2}{R^2} \right]. \quad (3.10)$$

The last step is to compute the flow rate ( $Q$ ) by integrating Equation (3.10)

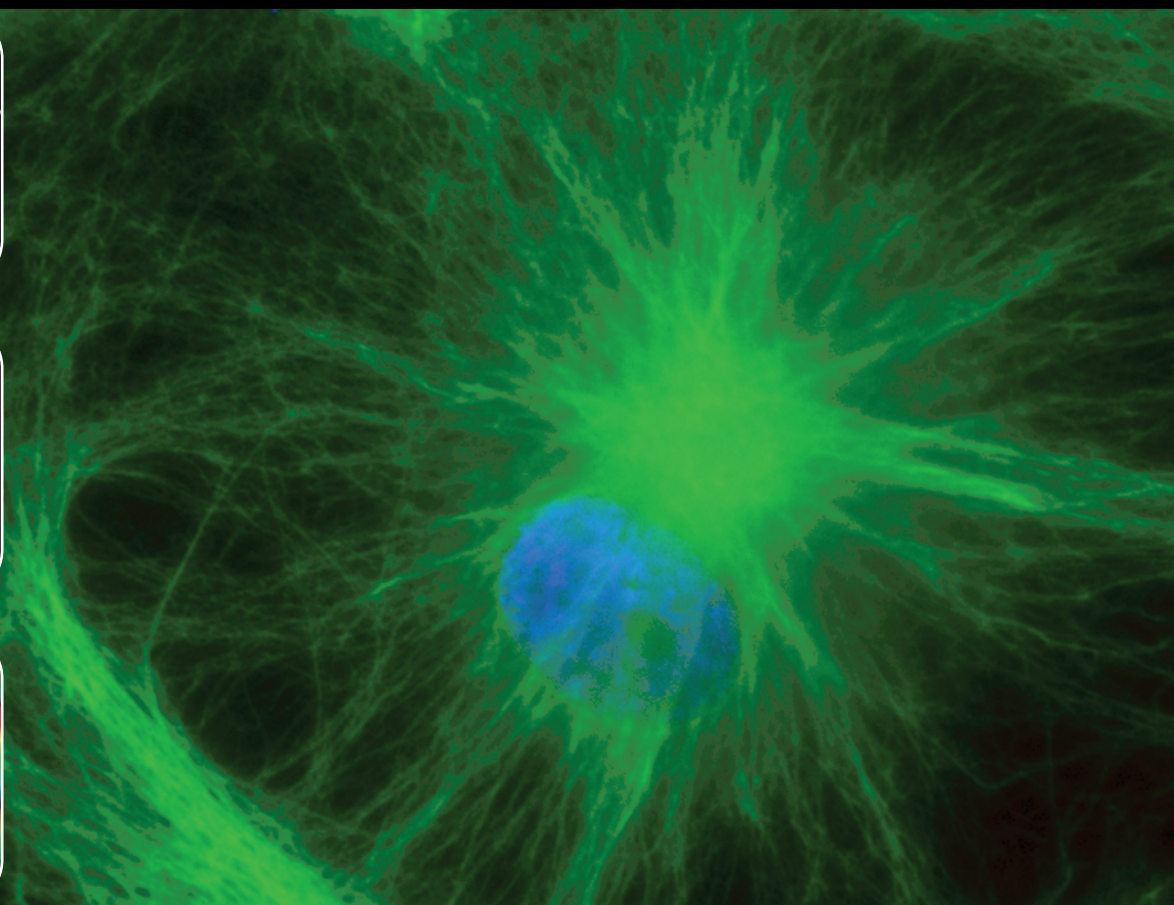
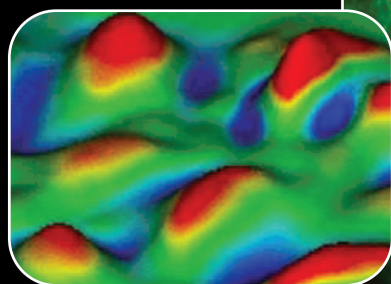
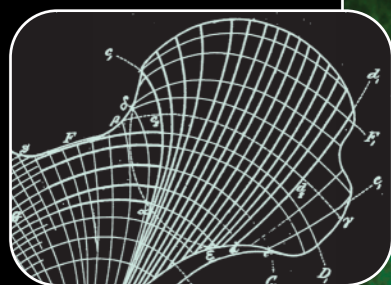
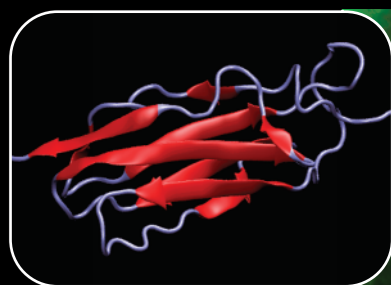
$$Q = -\frac{\pi R^4}{8\mu} \frac{dp}{dx}. \quad (3.11)$$

This is Poiseuille's law. Recognizing that the pressure gradient is constant and negative (for flow in the positive  $x$  direction), we can write  $-dp/dx = \Delta p/L$ , where  $\Delta p$  is the pressure drop over the tube length  $L$ .

CAMBRIDGE TEXTS IN  
BIOMEDICAL  
ENGINEERING

# Introductory **Biomechanics**

From Cells to Organisms



C. Ross Ethier and Craig A. Simmons